HETEROCYCLES, Vol. 65, No. 11, 2005, pp. 2605 - 2618
Received, 14th June, 2005, Accepted, 24th August, 2005, Published online, 26th August, 2005

NATURAL BOND ORBITAL ANALYSIS OF PERICYCLIC AND PSEUDOPERICYCLIC 1,5-ELECTROCYCLIZATIONS OF CONJUGATED AZIDES

Kazuaki Fukushima* and Hideo Iwahashi

Wakayama Medical University
811-1 Kimiidera, Wakayama, 641-8509, Japan
fuku@wakayama-med.ac.jp

Abstract – We have carried out calculations of energetic, structural and electronic properties for 1,5-electrocyclizations of conjugated azides at the B3LYP/6-31+G(d) level of theory. Analyses of the second-order perturbative energy lowering for interaction between donor and acceptor natural bond orbitals at the RHF/6-31+G(d) level of theory have revealed conjugated group dependent pericyclic and pseudopericyclic nature of the reactions.

INTRODUCTION

Reactivity of conjugated azides varies depending on the structure and electronic properties of the conjugated groups (Figure 1).[1] The reactivity of vinyl azides has been investigated from the experimental and the theoretical viewpoints. The vinyl azides undergo cyclization into 2*H*-azirines accompanying loss of N_2 (Figure 1a). An *ab initio* molecular orbital study showed that the ring closure and the extrusion of N_2 proceeded simultaneously.[2] It is worth noting that 1,5-electrocyclization into 1,2,3-triazole does not proceed. Imino azides are also reactive chemical intermediates, which undergo spontaneous 1,5-electrocyclizations to give 1,2,3,4-tetrazoles (Figure 1b). In this case, the 1,5-electrocyclization is more favorable than cyclization to three-membered compound accompanying loss of N_2. Reactivity of acyl azides is different from that of vinyl and imino azides (Figure 1c). Cyclization of acyl azides, which gives three- or five-membered heterocycles, does not proceed at ambient

temperature. Instead, pyrolysis of acyl azides yields isocyanates by migration of an alkyl group onto a nitrogen atom attached to a carbonyl group accompanying loss of N_2, which is known to be the Curtius rearrangement.[3]

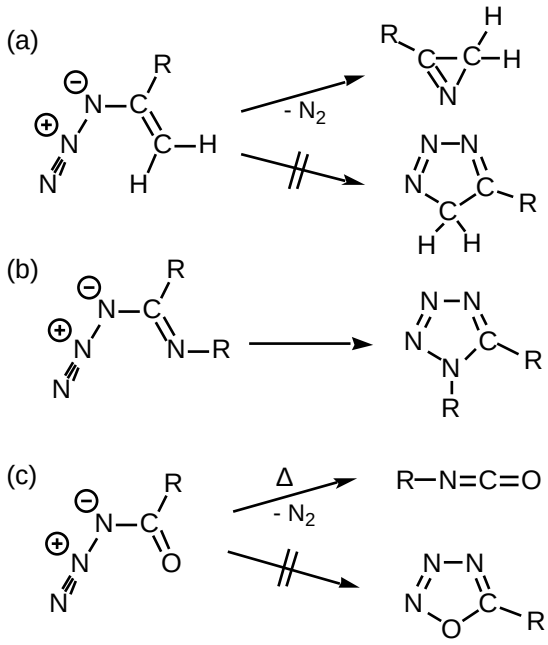

Figure 1. 1,5-Electrocyclizations of conjugated azides. (a) Reaction of vinyl azides gives 2*H*-azirine accompanying loss of N_2. 1,5-Electrocyclizations to 1,2,3-triazoles do not proceed. (b) 1,5-Electrocyclizations of imino azides give 1,2,3,4-tetrazoles. (c) The Curtius rearrangement of acyl azides gives isocyanates. Acyl azides do not cyclize to 1,2,3,4,-oxatriazoles.

In order to explain the conjugated group dependency of the reactivity of the conjugated azides, theoretical approaches have been carried out. Huisgen predicted the possibility of three types of mechanisms for the 1,5-electrocyclizations of conjugated 1,3-dipoles of the propargyl-allenyl types including the corresponding azide derivatives.[4] Leroy *et al.* performed *ab initio* calculations on 1,5-electrocyclizations of vinyl and imino azides at the STO-3G level.[5] They analyzed change of π-electron density along reaction pathway, and reported that the transition states of these reactions were different in the modes of interactions of the orbitals. The analysis suggested that in the cyclization of vinyl azide, π-electrons of the vinyl group participated in the formation of a new σ-bond, accompanying twisting at the end of the vinyl group. On the other hand, in the cyclization of imino azide, π-electrons of the imino group did not participate in the formation of a new σ-bond. The new σ-bond formation involved nucleophilic attack of lone pair electrons on the nitrogen atom of the imino group. The

imino group was not twisted during the in-plane approach of the imino-nitrogen toward the azide group.

The differences in reaction mechanisms on concerted reactions of unsaturated compounds containing heteroatoms were generalized in terms of the concept of *pericyclic and pseudopericyclic reactions.* The pseudopericyclic reactions were originally defined by Lemal *et al.* as one of the pericyclic reactions in which there is a disconnection in the cyclic array of overlapping orbitals, because of the presence of orthogonal orbital systems.[6] The concept of pericyclic and pseudopericyclic reactions has been developed and has successfully applied to electrocyclization, cycloaddition,[7a] sigmatropic rearrangement,[7b] and cheletropic reaction[7c] by Birney *et al.* They summarized general characteristics of the pseudopericyclic reactions as; (1) a pseudopericyclic reaction may be orbital symmetry allowed regardless of the number of electrons, (2) a barrier of a pseudopericyclic reaction can be very low, (3) a pseudopericyclic reaction will have a planar transition state.[7c]

Fabian *et al.* applied the concept to explaining 1,5-electrocyclization of conjugated diazomethanes and nitrile ylides (Figure 2).[8]

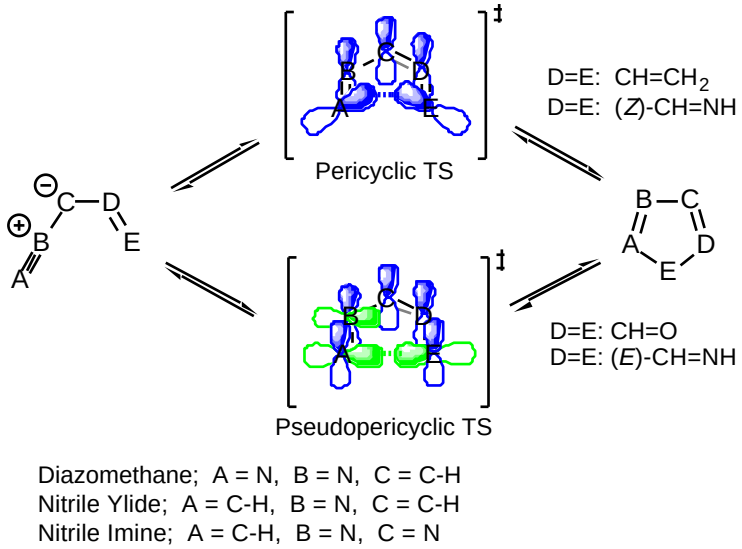

Figure 2. Pericyclic and pseudopericyclic mechanisms of 1,5-electrocyclizations of conjugated 1,3-dipoles of the propargyl-allenyl type.

The cyclizations of the vinyl and the (*Z*)-imino derivatives are pericyclic reactions, while those of the (*E*)-imino derivatives are pseudopericyclic reactions. Compared with these cases, determining the mechanisms of the cyclizations of formyldiazomethane and formyl nitrile ylide was not simple, since the formyl derivatives have only two or three hydrogen atoms, which were not effective structural probes for

determining the mechanisms. For determining the mechanisms of the cyclizations of the formyl derivatives, Fabian *et al*. analyzed the electronic properties such as natural populations and bond orders at the transition states, and compared them with those of the corresponding (*E*)-imino derivatives, of which reaction mechanisms were fully characterized by energetic and structural properties of the transition states.

We reported pericyclic and pseudopericyclic nature of the 1,5-electrocyclizations of conjugated nitrile imines (Figure 2).[9] The situations were similar to those of the conjugated diazomethanes and nitrile ylides. Thus, the mechanism of the cyclization of the formyl nitrile imine was not able to be determined based on only geometrical and energetic features of the transition state. For determining the mechanism of the reaction, we adopted analysis of the second-order perturbative energy lowering for interaction between donor and acceptor natural bond orbitals (NBOs) at each point on intrinsic reaction coordinates (IRCs) of the reactions. In this method, changes in interaction between NBOs are evaluated directly. This method revealed that the mechanisms of the 1,5-electrocyclizations were classified into two groups: the cyclizations of vinyl and (*Z*)-imino nitrile imines were pericyclic reactions, and those of formyl and (*E*)-imino nitrile imines were pseudopericyclic reactions.

Azide group consists of three nitrogen atoms and contains no C-H group. The geometrical information on the reaction mechanisms is much poorer compared to the reactions of the other conjugated 1,3-dipoles (diazomethanes, nitrile ylides, and nitrile imines). In this paper, we have determined mechanisms of the 1,5-electrocyclization of conjugated azides using analysis of the second-order perturbative energy lowering for interaction between donor and acceptor NBOs along IRCs of the reactions, which gives much information on the reaction mechanisms. The results obtained in this work have clearly explained the differences in reactivity of the conjugated azides.

COMPUTATIONAL METHODS

All calculations were performed using Gaussian 03W program.[10] Geometries were optimized at the B3LYP/6-31+G(d) level of theory.[11] All stationary points were characterized as minima or transition states by frequency calculations. IRC calculations were carried out at the B3LYP/6-31+G(d) level of theory to confirm that the obtained saddle points were the transition states of the 1,5-electrocyclizations of the conjugated azides. The NBO analyses[12] were performed at points on the IRCs at intervals of 0.05 amu$^{1/2}$Bohr at the RHF/6-31+G(d)//B3LYP/6-31+G(d) level of theory.

RESULTS AND DISCUSSION

Calculations were carried out for vinyl azide (**1a**), formyl azide (**1b**), (*Z*)-imino azide (**1c**), (*E*)-imino azide (**1d**), transition states of the 1,5-electrocyclizations (**2a** - **2d**), and five membered heterocycles (**3a** - **3c**(**3d**)) (Figure 3). Numberings of the atoms are also shown in Figure 3. In this paper, the numberings of **2** and **3** were analogous to **1**, to clarify the relationship of the atoms among these three chemical species.

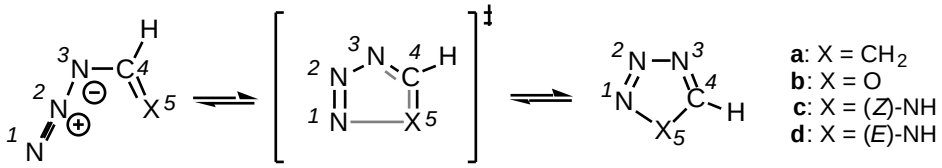

Figure 3. Structure and numbering of conjugated azides.

Energy. Conjugated azides react in various manners depending on the properties of the conjugated groups (Figure 1). The reactivity of the conjugated azides can be explained by energetics of the reactions.

Table 1. Relative Energies and Lowest Frequencies Calculated at the B3LYP/ 6-31+G(d) Level of Theory.

	E (kcal mol^{-1})*	$\tilde{\nu}$ (cm^{-1})
1a	0.00	173.3
2a	31.25	567.4i
3a	-4.57	379.5
1b	0.00	173.5
2b	18.05	270.6i
3b	15.78	569.3
1c	0.00	171.9
2c	27.99	757.6i
3c (**3d**)	-14.28	563.6
1d	0.00	180.7
2d	14.59	343.6i
3d (**3c**)	-11.65	563.6

* The energies are relative to those of the corresponding azide derivatives (**1a**-**1d**). The energies include zero-point vibrational energy (ZPVE), without scaling.

Calculated relative energies in regard to the corresponding azides (**1a** - **1d**), which include zero-point vibrational energy (ZPVE), are listed in Table 1. The relative energies along IRCs, which do not include

ZPVE, are shown in Figure 4.

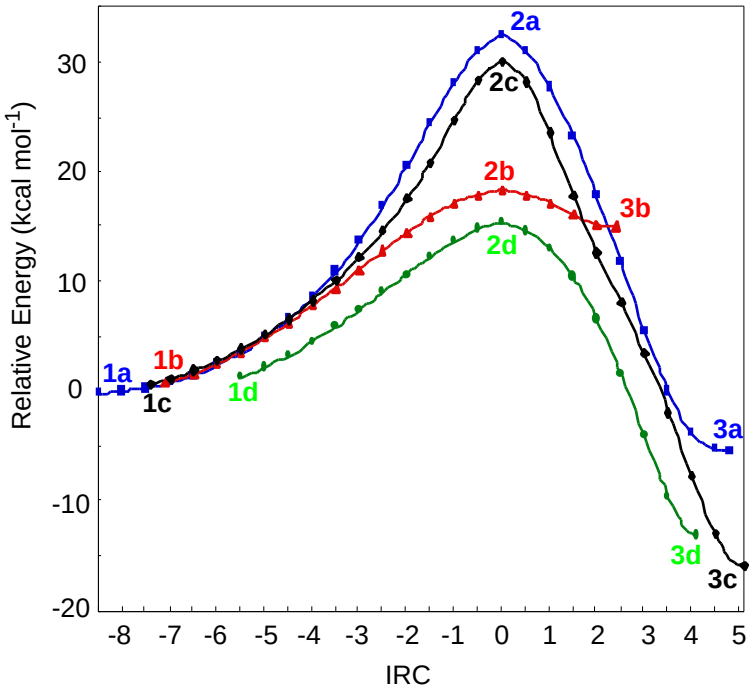

Figure 4. Energy profile of the reactions calculated at the B3LYP/6-31+G(d) level of theory.

Thermal reactions of vinyl azides usually give 2*H*-azirines accompanying loss of N_2. Formation of triazoles *via* 1,5-electrocyclization does not occur under the same conditions. The energy profile of the 1,5-electrocyclization from **1a** to **3a** shows that the reaction is not a favorable process. In the reaction from **1a** to **3a**, relative energy of the transition state (**2a**) was 31.25 kcal mol^{-1}. This indicates that the process is kinetically hindered by the high energy barrier, although it is exothermic by 4.57 kcal mol^{-1}. 1,5-Electrocyclizations of acyl azides are usually unfavorable processes. The energy profile of the 1,5-electrocyclization from **1b** to **3b** shows that **1b** is thermodynamically stable. The calculated energy barrier of the reaction (18.05 kcal mol^{-1}) was substantially lower than that for the cyclization of **1a** to **3a**. The energy change of the whole cyclization process from **1b** to **3b** was endothermic by 15.78 kcal mol^{-1}. The endothermicity of the cyclization from **1b** to **3b**, and the very low energy barrier (2.27 kcal mol^{-1}) of the reverse process (ring opening from **3b** to **1b**) indicate that the formation of **3b** is thermodynamically disadvantageous. Attempts to prepare imino azides were unsuccessful, since spontaneous ring closure gave 1,2,3,4-tetrazoles instead. The energy profile of cyclization from (*Z*)-imino azide **1c** to **3c** does not agree with the experimental results. The cyclization of **1c** was exothermic by 14.28 kcal mol^{-1}

with 27.99 kcal mol^{-1} of energy barrier. The energy profile indicates that the cyclization of **1c** does not proceed because of the high energy barrier in spite of the exothermicity of the reaction. On the other hand, the energy profile of cyclization from (*E*)-imino azide **1d** to **3d** can explain the experimentally observed spontaneous cyclizations of imino azides. The cyclization from **1d** to **3d** was exothermic by 11.65 kcal mol^{-1}, and the energy barrier is the lowest (14.59 kcal mol^{-1}) of the four model reactions of the conjugated azides (**1a** - **1d**). Both the kinetic and the thermodynamic factors facilitate the cyclization of **1d**.

Geometry. Optimized geometrical parameters of conjugated azides (**1a** - **1d**) are collected in Table 2. Geometrical features of all the conjugated azides were essentially identical. Azide groups were slightly bent at N2 with 172.7-174.1° of N1-N2-N3 angles. N1-N2 bonds (1.130-1.140 Å) are substantially shorter than N2-N3 bonds (1.240-1.255 Å), indicating triple bond character for the former bonds. All dihedral angles were 0° or 180°, indicating the molecules were completely planer.

Table 2. Bond Lengths (Å), Bond Angles (°), and Dihedral Angles (°) of Conjugated Azides (**1a** - **1d**) Optimized at the B3LYP/6-31+G(d) Level of Theory.

	1a	**1b**	**1c**	**1d**
N1-N2	1.140	1.130	1.137	1.132
N2-N3	1.240	1.255	1.244	1.251
N3-C4	1.415	1.417	1.428	1.408
C4-X5	1.340	1.210	1.270	1.273
N1-N2-N3	173.0	174.0	174.1	172.7
N2-N3-C4	117.9	114.8	117.1	115.5
N3-C4-X5	127.7	126.1	130.6	123.4
N1-N2-N3-C4	180.0	180.0	180.0	180.0
N2-N3-C4-X5	0.0	0.0	0.0	0.0
N3-C4-X5-H5in	0.0	–	0.0	–
N3-C4-X5-H5out	180.0	–	–	180.0

Optimized structures and geometrical parameters of transition states for the reactions are depicted in Figure 5. In the optimized structures of **2a** - **2d**, N2-N3 bonds were longer and N3-C4 bonds were shorter compared to the corresponding azides (**1a** - **1d**). N1-N2-N3 angles of **2a** - **2d** were smaller than those of **1a** - **1d**, which reflects increasing interaction between N1 and X5. Dihedral angles of the transition states show that **2b** and **2d** are completely planer, while **2a** and **2c** are not. The dihedral angles of N3-C4-X5-$H5_{in}$ and N3-C4-X5-$H5_{out}$ show that C4-X5 bonds are twisted in **2a** and **2c** and the bond is not twisted in **2d**. Thus there are two modes in the transition states of the reactions; **2a** and **2c** are

monorotatory modes and **2d** is a nonrotatory mode. The twisting of the C4-X5 bonds in **2a** and **2c** indicates that π-electrons at X5 participate in the formation of the N1-X5 σ-bonds. The planer conformation of the C4-N5 bond in **2d** indicates that in-plane nucleophilic attack of the lone pair electrons at N5 lead to the formation of the N1-N5 bond. The optimized geometry of **2b** is less informative on the mechanism of the cyclization. Although the complete planer conformation of **2b** is similar to that of **2d**, the mode of the cyclization of **2b** cannot be determined based on only the geometrical information, since there is no decisive structural probe for the twisting in the C4-O5 bond.

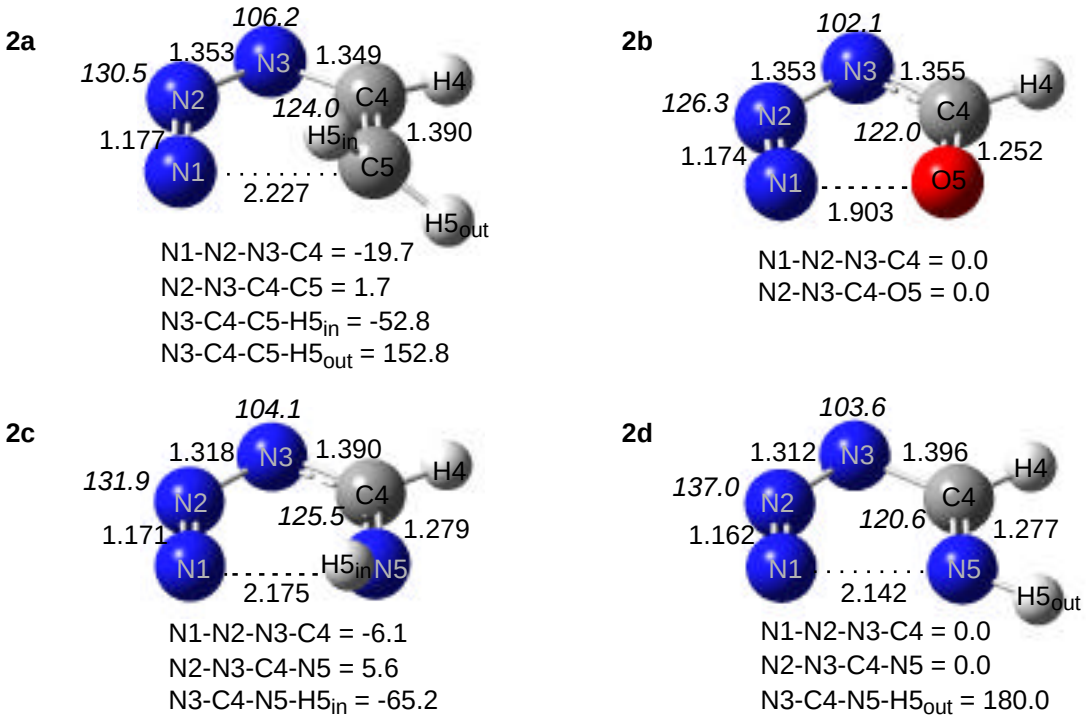

Figure 5. Bond lengths (Å), bond angles (°, *in italics*), and dihedral angles (°) of transition states (**2a** - **2d**) optimized at the B3LYP/6-31+G(d) level of theory.

The geometrical parameters of heterocycles (**3**) are listed in Table 3. All of the heterocycles had planer N1-N2-N3-C4-X5 frameworks. There was bond alternation in the geometry of **3a**, which is typical in non-aromatic cyclic unsaturated compounds. Bond alternation was reduced in **3b** and **3c** (**3d**) because of increase in aromatic character of the two molecules.

Table 3 Bond Lengths (Å), Bond Angles (°), and Dihedral Angles (°) of Heterocycles (**3a** - **3d**) Optimized at the B3LYP/6-31+G(d) Level of Theory.

	3a	**3b**	**3c(3d)**
N1-N2	1.244	1.247	1.292
N2-N3	1.482	1.384	1.365
N3-C4	1.282	1.301	1.317
C4-X5	1.490	1.322	1.348
N1-X5	1.467	1.451	1.353
N1-N2-N3	111.9	112.9	111.3
N2-N3-C4	105.5	103.5	105.8
N3-C4-X5	111.4	114.0	108.3
C4-X5-N1	101.4	103.2	108.6
X5-N1-N2	109.8	106.4	106.0
N1-N2-N3-C4	0.0	0.0	0.0
N2-N3-C4-X5	0.0	0.0	0.0
N3-C4-X5-H5in	117.7	–	180.0
N3-C4-X5-H5out	117.7	–	180.0
N3-C4-X5-N1	0.0	0.0	0.0
C4-X5-N1-N2	0.0	0.0	0.0
X5-N1-N2-N3	0.0	0.0	0.0

NBO Analysis. Figure 6 illustrates notation of NBOs and schematic diagram of the second-order perturbative energy lowering ($\Delta E_{i,j}^{(2)}$) for interaction between donor and acceptor NBOs.

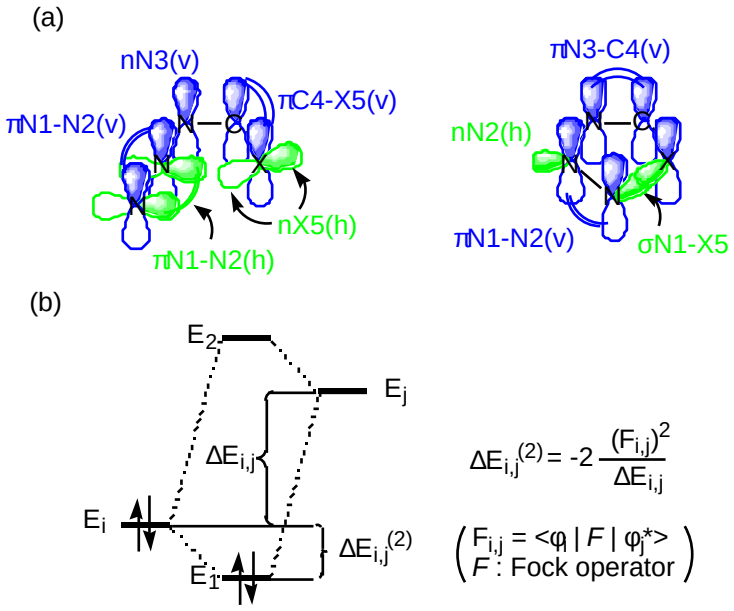

Figure 6. (a) Names of Natural Bond Orbitals (NBOs). (b) Schematic diagram of the second-order energy-lowering ($\Delta E_{i,j}^{(2)}$) for interaction betweendonor and accepter NBOs.

Figures 7 and 8 summarize changes in $\Delta E_{i,j}^{(2)}$ along IRCs of the 1,5-electrocyclizations. In vinyl azide (**1a**), large $\Delta E_{i,j}^{(2)}$ value for electron-donating interaction nN3(v) → π*N1-N2(v) suggests strong delocalization of nN3(v) in the azide group. The nN3(v) was also delocalized at the vinyl group. In the process from **1a** to **2a**, the nN3(v)→π*N1-N2(v) interaction was suddenly decreased near **2a**. Instead, nN3(v)→π*N1-N2(h) interaction increased near **2a**, which indicated that N1-N2 moiety were twisted near the transition state. Electron-donating interaction πC4-C5(v)→π*N1-N2(h) also increased at **2a** (14.77 kcal mol^{-1}), indicating the interaction lead to the formation of σ-bond between N1 and C5.

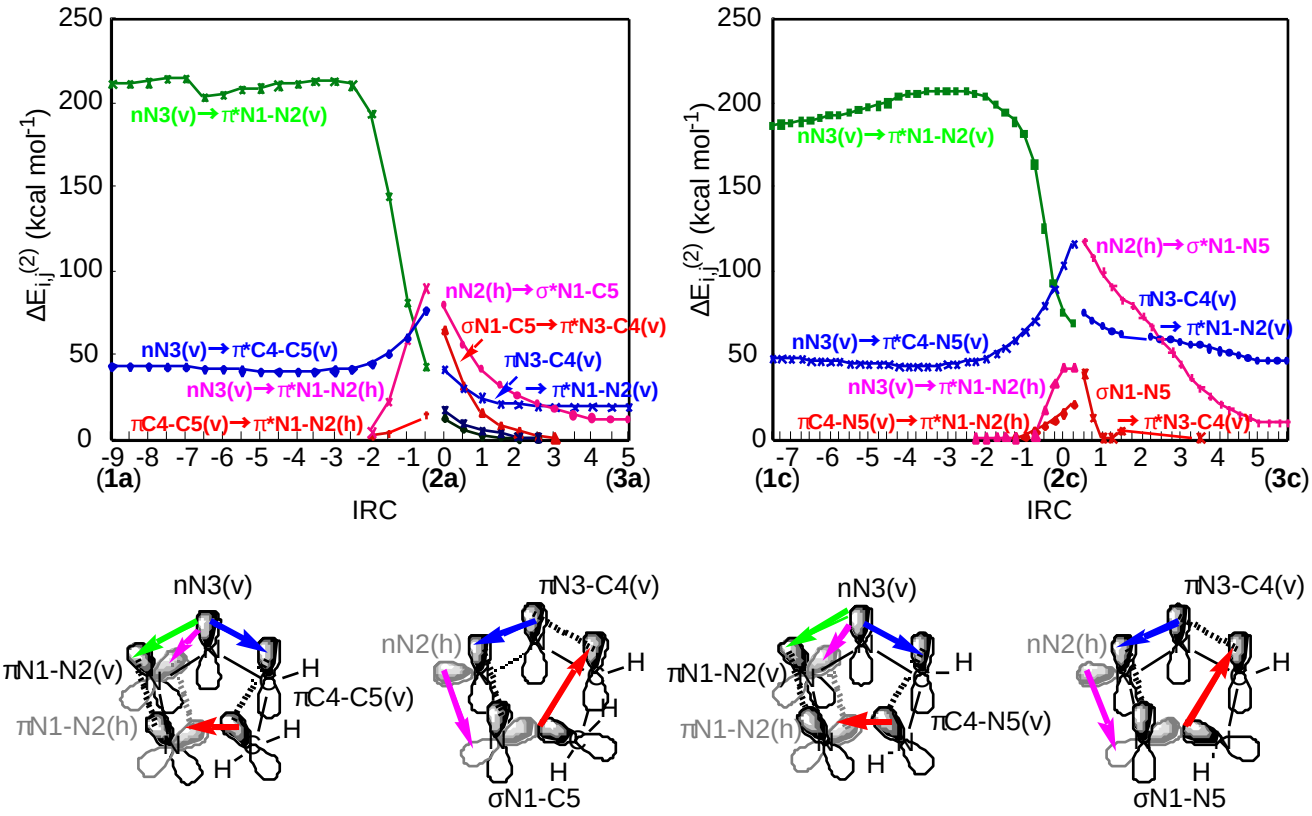

Figure 7. Changes in the second-order energy lowering ($\Delta E_{i,j}^{(2)}$) by electron-donating interaction between donor and acceptor NBOs along intrinsic reaction coordinates (IRCs) of the 1,5-electro-cyclizations from **1a** to **3a** and from **1c** to **3c**.

In the process from **2a** to **3a**, some electron-donating interactions such as nN2(h)→σ*N1-C5 and σN1-C5 →π*N3-C4(v) were decreasing as the cyclization proceeded. These interactions play an important role at the transition state of the reverse process from **3a** to **2a**. Thus in the ring opening reaction from **3a** to **1a**, the electron-donation from nN2(h) increase the electron density of σ*N1-C5, and that from σN1-

C5 to π*N3-C4(v) decrease the electron density of the σN1-C5 bond. The combination of the two interactions results in the break of the σN1-C5 bond in the ring opening process. The energy profiles of $\Delta E_{i,j}^{(2)}$ in the reaction **1c** ⇄ **3c** were similar to those of **1a** ⇄ **3a**. The similarity in changes of electron-donation pattern along IRC indicates the mechanisms of both the reactions are able to classified into the same group.

The energy profiles of $\Delta E_{i,j}^{(2)}$ along IRC for the reaction **1b** ⇄ **3b** show different features from the former ones.

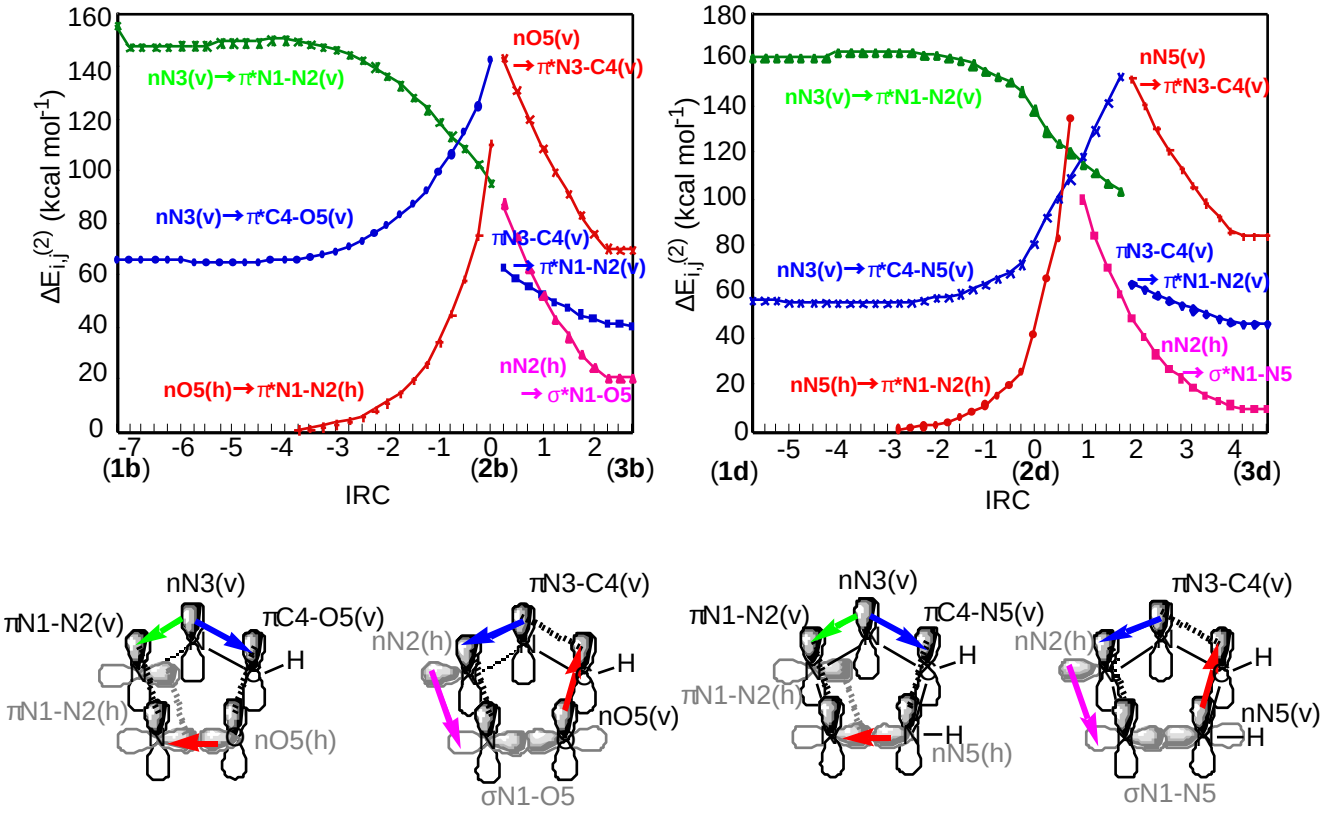

Figure 8. Changes in the second-order energy lowering ($\Delta E_{i,j}^{(2)}$) by electron-donating interaction between donor and acceptor NBOs along intrinsic reaction coordinates (IRCs) of the 1,5-electro-cyclizations from **1b** to **3b** and from **1d** to **3d**.

In the process from **1b** to **2b**, electron-donating interaction from nN3(v) to π*N1-N2(v) decreased near **2b**. Decrease in the nN3(v)→π*N1-N2(v) interaction in the process **1a**→**2a** (or **1c**→**2c**) was caused by twisting in the azide group, which was accompanied by increment of the nN3(v)→π*N1-N2(h) interaction. The decrease in the nN3(v)→π*N1-N2(v) interaction in the process **1b**→**2b** was not

caused by twisting in the azide group, because there was no increment of the nN3(v)→π*N1-N2(h) interaction. Thus, the lone pair electron nN3(v) was strongly delocalized at the formyl group (C4=O5) near the transition state (**2b**).

In this process, the electron-donation nO5(h)→π*N1-N2(h) increased near **2b**. The $\Delta E_{i,j}^{(2)}$ for the interaction was 110.74 kcal mol^{-1} at **2b**, which was much larger than the $\Delta E_{i,j}^{(2)}$ for the bond forming interactions πC4-C5(v)→π*N1-N2(h) at **2a** (14.77 kcal mol^{-1}) and **2c** (15.11 kcal mol^{-1}). The difference is due to the degree of overlapping of the orbitals. In-line alignment of the interacting orbitals at **2b** is more effective for the electron-donating interaction than parallel (or distorted parallel) alignment of the p-orbitals at **2a** and **2c**. These electron-donation manner at the transition state, indicate the ring closure proceeds by in-plane electron-donating interaction from nO5(h) to π*N1-N2(h), and there is no bond twisting at both ends of the molecule. In the reverse process form **3b** to **2b**, the electron-donation from nN2(h) to σ*N1-O5 increased, while there was no electron-donating interaction from σN1-O5 to π*N3-C4 (v). Thus in the reaction **1b** $\rightleftarrows$ **3b**, the bond-forming and bond-breaking interactions between N1 and O5 proceed within the mean molecular plane, and there was no bond twisting at both ends of the molecule. The interactions between nN3(v) and π*N1-N2(v), nN3(v) and π*C4-O5(v), nO5(v) and π*N3-C4(v), and πN3-C4(v) and π*N1-N2(v) are orthogonal to the mean molecular plane, and are consequently independent to the bond forming interactions between N1 and O5. The energy profiles of $\Delta E_{i,j}^{(2)}$ in the reaction **1d** $\rightleftarrows$ **3d** were similar to those of **1b** $\rightleftarrows$ **3b**.

CONCLUSION

The 1,5-electrocyclizations of conjugated azides (**1a**-**1d**) are classified into two groups (Figure 9). The cyclizations of vinyl azide (**1a**) and (*Z*)-imino azide (**1c**) are categorized in the same group. These cyclizations are *pericyclic reactions*, in which π-electrons on N1 to X5 interact in concerted manner during the reaction. The energy barriers of these reactions are substantially high. At the transition states (**2a** and **2c**), the C4-X5 bonds are twisted, indicating that π-electrons at the C4-X5 bonds interact with the π*N1-N2 orbitals. The forming N1-X5 bonds interact with the π*N3-C4 orbitals just after passing the transition states (**2a** and **2c**) in the cyclization processes.

The cyclizations of formyl azide (**1b**) and (*E*)-imino azide (**1d**) are categorized in the other group.

These reactions show some typical characteristics of *pseudopericyclic reactions*. The energy barriers of the cyclizations of **1b** and **1d** are low. At the transition states (**2b** and **2d**), the C4-X5 bonds are not twisted, and lone pair electrons at X5 interact with the π*N1-N2 (h) orbitals. The large $\Delta E_{i,j}^{(2)}$ values for these interactions may contribute to the relative low activation energy of the reactions to some extent. The formations of the N1-X5 bonds proceed by in-plane interactions of the orbitals. There are the other type of the interactions among π-orbitals on N1, N2, N3, C4, and X5. These interactions occur out of the mean molecular planes, and are orthogonal to the in-plane interactions between N1 and X5. Thus, there are disconnections between the in-plane and the out-of-plane interactions.

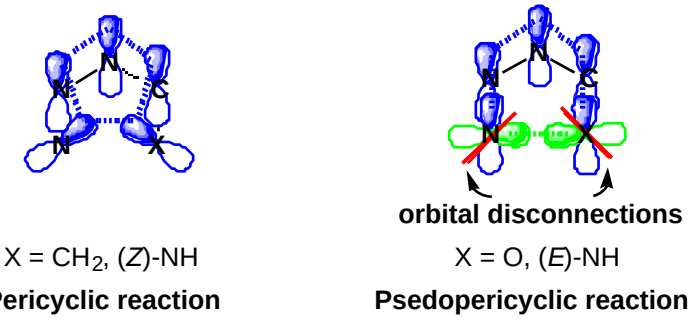

Figure 9. Orbital interactions in pericycic and pseudopericyclic reactions.

In this work, we have determined the mechanisms of 1,5-electrocyclizations of conjugated azides (**1a**-**1d**) by analysis of the second-order perturbative energy-lowering ($\Delta E_{i,j}^{(2)}$) for the interaction between donor and acceptor NBOs, as well as energetics and the geometrical features at each point on IRCs. This method is effective for analysis of reaction mechanisms, where reactants and products have no informative structural probe for the mechanisms.

REFERENCES

1. E. C. Taylor and I. J. Turchi, *Chem. Rev.*, 1979, **79**, 181.
2. T. Yamabe, M. Kaminoyama, T. Minato, K. Hori, K. Isomura, and H. Taniguchi, *Tetrahedron*, 1984, **40**, 2095.
3. (a) T. Curtius, *Chem. Ber.*, 1890, **23**, 3023; (b) P. A. S. Smith, *Org. React.*, 1946, **3**, 337; (c) D. V. Banthorpe, 'The Chemistry of the Azido Group,' ed. by S. Patai, Interscience, New York, 1971, pp. 397-405.

4. R. Huisgen, *Angew. Chem. Int. Ed. Engl.*, 1980, **19**, 947.

5. (a) L. A. Burke, J. Elguero, G. Leroy, and M. Sana, *J. Am. Chem. Soc.*, 1976, **98**, 1685; (b) L. A. Burke, G. Leroy, M. T. Nguyen, and M. Sana, *J. Am. Chem. Soc.*, 1978, **100**, 3668.

6. J. A. Ross, R. P. Seiders, and D. M. Lemal, *J. Am. Chem. Soc.*, 1976, **98**, 4325

7. (a) D. M. Birney and P. E. Wagenseller, *J. Am. Chem. Soc.*, 1994, **116**, 6262; (b) D. M. Birney, X. Xu, and S. Ham, *Angew. Chem. Int. Ed.*, 1999, **38**, 189; (c) D. M. Birney, S. Ham, and G. R. Unruh, *J. Am. Chem. Soc.*, 1997, **119**, 4509.

8. (a) W. M. F. Fabian, V. A. Bakulev, and C. O. Kappe, *J. Org. Chem.*, 1998, **63**, 5801; (b) W. M. F. Fabian, C. O. Kappe, and V. A. Bakulev, *J. Org. Chem.*, 2000, **65**, 47.

9. K. Fukushima and H. Iwahashi, *Bull. Chem. Soc. Jpn.*, 2004, **77**, 1671.

10. Gaussian 03, Revision C.02, M. J. Frisch, G. W. Trucks, H. B. Schlegel, G. E. Scuseria, M. A. Robb, J. R. Cheeseman, J. A. Montgomery, Jr., T. Vreven, K. N. Kudin, J. C. Burant, J. M. Millam, S. S. Iyengar, J. Tomasi, V. Barone, B. Mennucci, M. Cossi, G. Scalmani, N. Rega, G. A. Petersson, H. Nakatsuji, M. Hada, M. Ehara, K. Toyota, R. Fukuda, J. Hasegawa, M. Ishida, T. Nakajima, Y. Honda, O. Kitao, H. Nakai, M. Klene, X. Li, J. E. Knox, H. P. Hratchian, J. B. Cross, V. Bakken, C. Adamo, J. Jaramillo, R. Gomperts, R. E. Stratmann, O. Yazyev, A. J. Austin, R. Cammi, C. Pomelli, J. W. Ochterski, P. Y. Ayala, K. Morokuma, G. A. Voth, P. Salvador, J. J. Dannenberg, V. G. Zakrzewski, S. Dapprich, A. D. Daniels, M. C. Strain, O. Farkas, D. K. Malick, A. D. Rabuck, K. Raghavachari, J. B. Foresman, J. V. Ortiz, Q. Cui, A. G. Baboul, S. Clifford, J. Cioslowski, B. B. Stefanov, G. Liu, A. Liashenko, P. Piskorz, I. Komaromi, R. L. Martin, D. J. Fox, T. Keith, M. A. Al-Laham, C. Y. Peng, A. Nanayakkara, M. Challacombe, P. M. W. Gill, B. Johnson, W. Chen, M. W. Wong, C. Gonzalez, and J. A. Pople, Gaussian, Inc., Wallingford CT, 2004.

11. A. D. Becke, *J. Chem. Phys.*, 1993, **98**, 5648.

12. (a) NBO Version 3.1, E. D. Glendening, A. E. Reed, J. E. Carpenter, and F. Weinhold; (b) A. E. Reed, L. A. Curtiss, and F. Weinhold, *Chem. Rev.*, 1988, **88**, 899.